Online Oxygen Kinetic Isotope Effects Using Membrane Inlet Mass Spectrometry Can Differentiate between Oxidases for Mechanistic Studies and Calculation of Their Contributions to Ox…

ARTICLE *in* ANALYTICAL CHEMISTRY · MAY 2014

Impact Factor: 5.64 · DOI: 10.1021/ac501086n · Source: PubMed

7 AUTHORS, INCLUDING:

Mun Hon Cheah
Australian National University
21 PUBLICATIONS **445** CITATIONS
SEE PROFILE

David Alexander Day
Flinders University
245 PUBLICATIONS **10,188** CITATIONS
SEE PROFILE

Justine P Roth
Johns Hopkins University
55 PUBLICATIONS **1,241** CITATIONS
SEE PROFILE

analytical chemistry

Article

pubs.acs.org/ac

Online Oxygen Kinetic Isotope Effects Using Membrane Inlet Mass Spectrometry Can Differentiate between Oxidases for Mechanistic Studies and Calculation of Their Contributions to Oxygen Consumption in Whole Tissues

Mun Hon Cheah,*[,†] A. Harvey Millar,[‡] Ruth C. Myers,[‡] David A. Day,[§] Justine Roth,[⊥] Warwick Hillier,[†] and Murray R. Badger*[,†,¶]

[†]Division of Plant Science, Research School of Biology, the Australian National University, Canberra ACT 0200, Australia

[¶]The ARC Centre of Excellence for Translational Photosynthesis, the Australian National University, Canberra ACT 0200, Australia

[‡]The ARC Centre of Excellence in Plant Energy Biology, The University of Western Australia, 35 Stirling Highway, Crawley, Perth, Western Australia 6009, Australia

[§]Flinders University, Bedford Park, Adelaide, South Australia 5042, Australia

[⊥]Department of Chemistry, The Johns Hopkins University, 3400 North Charles Street, Baltimore, Maryland 21218, United States

Supporting Information

ABSTRACT: The reduction chemistry of molecular oxygen underpins the energy metabolism of multicellular organisms, liberating free energy needed to catalyze a plethora of enzymatic reactions. Measuring the isotope signatures of ^{16}O and ^{18}O during O_2 reduction can provide insights into both kinetic and equilibrium isotope effects. However, current methods to measure O_2 isotope signatures are time-consuming and disruptive. This paper describes the application of membrane inlet mass spectrometry to determine the oxygen isotope discrimination of a range of O_2-consuming reactions, providing a rapid and convenient method for determining these values. A survey of oxygenase and oxidase reactions provides new insights into previously uncharacterized amino acid oxidase enzymes. Liquid and gas phase measurements show the ease of assays using this approach for purified enzymes, biological extracts and intact tissues.

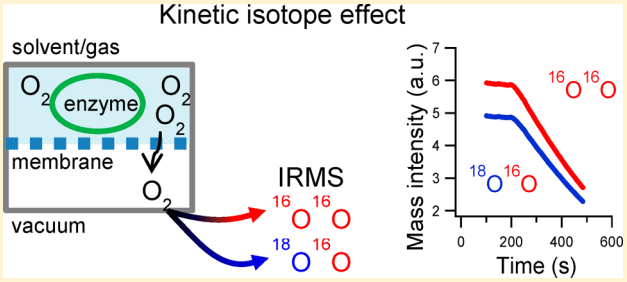

The oxygenation of earth's atmosphere, commencing ~2.5 billion years ago, has been the most important driving force in shaping the evolution of aerobic life forms. Increasing O_2 concentrations have been correlated with expanded diversity and complexity of biochemical reactions. As the atmospheric conditions became more abundant in O_2, a range of redox reactions were harnessed with O_2 as the major acceptor for electron fluxes in biology using enzymes such as the oxidases, which use O_2 as the electron sink and the oxygenases, which insert one atom from O_2 into the substrate while the second O atom is reduced to water. Generally, the activation of O_2 is achieved via mechanisms that involve a series of electron transfers coupled to proton transfers, as indicated by ^{18}O kinetic isotope effects and computational studies.[1,2]

Advances in crystallographic and spectroscopic characterization have provided some insights into active site processes. However, detailed understanding of mechanisms and the control and selectivity of reaction rates have remained a challenge. Consequently, there has been considerable impetus to develop other approaches to understand the kinetics of reaction mechanisms and among these, methods that can examine and measure O_2 (^{18}O) isotope effects have been of particular importance.[2−5] Because the ^{18}O isotope effects reflect the change in bond organization during the reaction, they provide information that can be used to evaluate the intrinsic barriers and provide information needed to understand oxidase and oxygenase reactions.

Apart from understanding reaction mechanisms, quantifying the rates of different O_2 consuming reactions in active biological tissues has also been of great interest to understand metabolic flux and partitioning. This has been particularly so for the processes of respiration and photosynthesis. An example of this is found in the study of plant respiration, where two terminal oxidase enzyme complexes, cytochrome *c* oxidase (CcO) and the di-iron alternative oxidase (AOX), compete for electrons in the mitochondrial electron transport chain where each are coupled to different efficiencies of ATP synthesis through the plant respiratory process.[6−8] The fact that they

Received: March 25, 2014
Accepted: April 4, 2014

   dx.doi.org/10.1021/ac501086n | *Anal. Chem.* XXXX, XXX, XXX−XXX

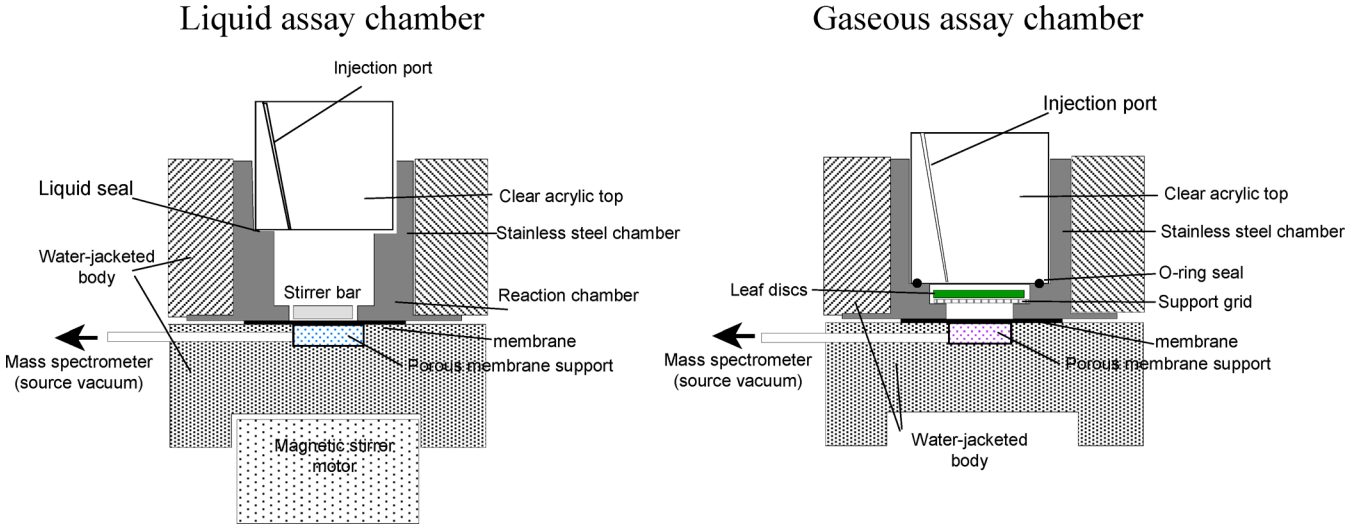

Figure 1. Diagrams of liquid and gaseous reaction cuvettes used for oxygen consuming reactions. The cuvettes are designed to seal the reaction from the external atmosphere and admit a sample of the gases from the reaction to the mass spectrometer via a gas-permeable plastic membrane in the base of the cuvette. Volume of the gas cuvette is typically 1 mL, while the liquid cuvette is 4 mL. The liquid cuvette is stirred with a magnetic stir bar to reduce the boundary layer resistance next to the plastic membrane.

show different heavy ^{18}O isotope fractionation has enabled differential fluxes to be determined in vivo.[6−8] Plant photosynthesis is also associated with a number of simultaneously occurring O_2 consuming reactions including ribulose-1,5-bisphosphate carboxylase/oxygenase (RuBisCO), glycolate oxidase and the Mehler reaction,[9,10] which operate simultaneously with mitochondrial respiration in plant tissues in the light. Although some differences in ^{18}O isotope effects have been identified in these reactions,[11] solving the rates of individual reactions is much more problematic in these systems and accurately measuring flux along all these pathways has not been achieved.

The study of kinetic ^{18}O isotope effects with enzymes and biological tissues can be performed in both liquid and gaseous phase reactions and different technical difficulties are associated with each. In general, both methods are performed using the natural abundance of O_2 isotopologues, $^{16,16}O_2$ (mass 32) and $^{16,18}O_2$ (mass 34), present in the same reaction. Detection is based on a multiple collector magnetic sector isotope-ratio mass spectrometer (IRMS). Usually, experiments involve measuring the change in the ratio of isotopologues remaining after O_2 consumption in a closed reaction vessel. For gaseous reactions, current methods involve periodic sampling of the gaseous atmosphere using a sampling loop connected to a GC inlet connected in turn to an IRMS.[10,12] For liquid reactions, the protocol is more laborious and error prone. Liquid samples are taken at various time points and O_2 is extracted from the solution followed by passage through a number of cold traps under vacuum and then converted to CO_2 for isotope analysis by the IRMS.[5,8,10] In particular, the liquid procedure can be laborious and it may take several hours for an analysis of a single reaction duration to be completed.

This paper describes the development of an alternative procedure to study the O_2 kinetic isotope effects (KIE) of both liquid and gaseous O_2 consuming reactions using membrane inlet mass spectrometry (MIMS). The advantage of the approach is that the isotope ratio measurements are made within the time frame of each reaction, which may be a short as 5 min, achieving similar precision to the previous techniques but with much greater simplicity, speed and utility with respect to studying O_2 consuming processes. Measurements with the MIMS isotope ratio magnetic sector system enables several O_2 isotopologues (i.e., $^{16,16}O_2$, $^{16,18}O_2$ and $^{18,18}O_2$) to be simultaneously measured and without any prior gas manipulations, transfers or reprocessing, and purification. In this paper, we compare existing values in the literature with the MIMS approach and have analyzed ^{18}O isotope effects for several previously unreported reactions. Of significant interest is the discovery of an unusually high discrimination value/^{18}O kinetic isotope effect for D- and L-amino acid oxidase enzymes, suggesting a mechanism not considered in existing studies of flavoprotein reactivity and very distinct from measurements of a range of oxygenases and flavin and di-iron oxidases.

MATERIALS AND METHODS

Mass Spectrometer Assay and Instrumentation. Measurements of changes in the concentrations of oxygen isotopes were performed in two cuvettes designed for monitoring either liquid or gaseous reactions (see Figure 1). The MIMS cuvette was fabricated from stainless steel and consists of two parts. The reaction chamber, located at the top part of the cuvette, is formed by pressing a semipermeable polymer membrane (approximately 25 × 25 mm, supported by a 10.5 mm diameter circular porous polyethylene frit, Bel-Arts Products) between the top and bottom part. The mating surfaces of both parts are polished to a mirror finish. The bottom part is connected to the inlet of the mass spectrometer via 1/8 in. stainless steel tubing and all fittings and valves are sourced from Swagelok. A water trap cooled by ethanol/dry ice was built between the cuvette and mass spectrometer inlet from the same materials. Gases from the reaction chamber are transported to the vacuum of the mass spectrometer inlet via the semipermeable membrane through a process known as pervaporation. The reaction chamber of the sample cuvette (Figure 1) was sealed from the atmosphere during the reaction by either liquid or O-ring seals formed with the acrylic top, and in the case of the gas chamber, the injection port was sealed with plastic [Blu-Tack] putty during the reaction to prevent

dx.doi.org/10.1021/ac501086n | Anal. Chem. XXXX, XXX, XXX−XXX

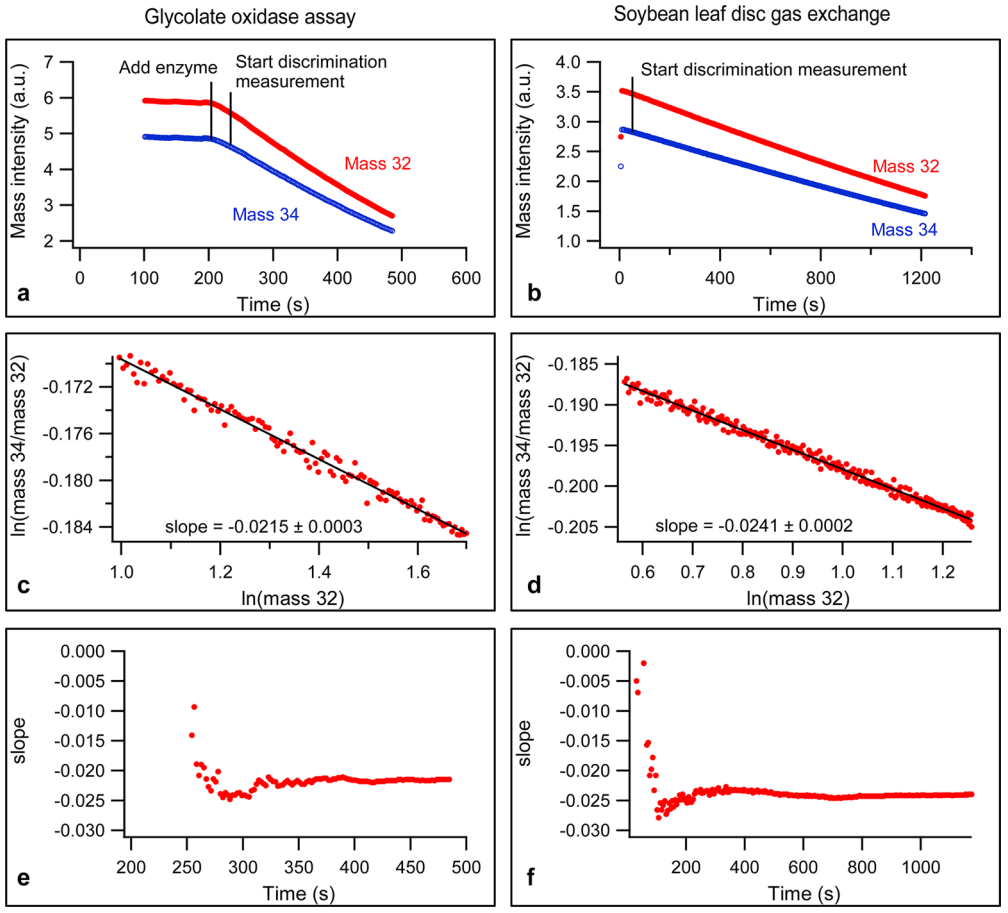

Figure 2. Time courses for sample liquid (glycolate oxidase) and gaseous (soybean leaf disc respiration) oxygen consuming reactions. (a,b) The time courses for each reaction with masses 32 and 34 shown. Note that mass 34 is shown at about 200× the sensitivity of mass 32 due to the differences in natural isotope abundance. Liquid reactions were started by addition of enzyme while gaseous reactions were started some time after sealing the cuvette containing the leaf discs. The analysis start points are indicated on the time courses. (c,d) Replot of the reaction data from the point where the discrimination measurement is started as discussed in the text as ln(mass 34/mass 32) vs ln(mass 32). (e,f) The slope values obtained for the plots in Figure 2c,d as the data is accumulated during the time course.

external gas exchange. Both the bottom and top sections of the cuvette were temperature controlled by a water jacket, to stabilize both the reaction rate and the gas permeability of the membrane. For the liquid chamber, the reaction was continuously stirred with a magnetic stir bar. In the gas chamber, circular leaf pieces were supported by stainless steel grids and multiple discs were used for each assay. Limiting the amount of gas consumed via the membrane was particularly important during the liquid assay and is controlled by the membrane material, thickness and surface area. The semi-permeable membrane is either a low density polyethylene (LDPE) film (ca. 43 μm thick) or perfluoroalkoxy (PFA) film (ca. 58 μm thick) and the surface area is defined by the bottom opening of the reaction chamber (86.6 mm^2). The choice of membrane material and thickness where selected such that there is minimal consumption of gas while maintaining sufficient signal intensity in the mass spectrometer.

Measurements of the concentrations of $^{16,16}O_2$ (mass 32) and $^{16,18}O$ (mass 34) were made using a purpose-built Isoprime IRMS that was interfaced to a membrane inlet for gas sampling (MicroMass Instruments Ltd.). The magnetic sector instrument utilized an 8-cup collector array enabling multiplexing of 8 simultaneous mass peaks including masses 32, 34 and 44. Data collection was further customized with in-house data acquisition software and hardware. The software developed for/on Visual Basic (Microsoft) enabled real time global analysis of isotopic signals, gas concentrations and, in this application, isotopic fractionation. The hardware platform was developed with high speed counters to read the frequency outputs of the head amplifier directly. The design enabled all data to be collated and evaluated in real time. Each data point typically represented a bin of 5 s of continuous data measurement and thus is extensively oversampled. Measurements on the mass 32 and mass 34 collectors were made with 10^9 and 10^{11} ohm resistors, respectively. During assays, the source pressure was around 8×10^{-8} Torr and filament current on the mass spectrometer was 100 μamps. A second equivalent IRMS (Delta V advantage Thermo Electron GmbH) was also used to independently validate the approach with identical findings to the Isoprime system.

Assay Procedures. Liquid and gaseous O_2 consumption assays were conducted in the reaction cuvettes (Figure 1) and sample data for reaction durations are shown (Figure 2). The liquid assays were conducted in a manner where all components needed for the assay, except enzymes, were added to the closed reaction cuvette and the background O_2 signals for masses 32 and 34 allowed to stabilize. The reactions were initiated with the injection of a small volume (typically in the microliter range) of concentrated enzyme. Significant decreases in the O_2 mass 32 and 34 signals are reported by the

dx.doi.org/10.1021/ac501086n | Anal. Chem. XXXX, XXX, XXX−XXX

mass spectrometer (Figure 2a). For assays in the gas phase, the material to be measured is placed on a stainless steel grid above the plastic membrane inlet, the cuvette closed and O_2 consumption measured when a steady rate of O_2 decline had been established. In the gas assay, membrane consumption did not contribute significantly to gas decline. For both assays, it is important to establish reaction conditions in which 20−50% of the initial O_2 substrate is consumed during the period of the assay (see discussion on consumption of O_2 by membrane below). For liquid assays, this generally occurred over a 5−15 min period, while for gas reactions, this was 10−40 min depending on tissue activity. Because of the significantly larger amount of O_2 per unit volume in gas assays, it is crucial to maximize the tissue to volume ratio so that sufficient consumption can be achieved in the desired time and the use of a small 1 mL cuvette aided this. For liquid assays, the major consideration was to reduce the membrane consumption per total assay volume; hence 4 mL assays were employed.

It should be noted that if lower enzyme activities are used, background membrane fractionation values begin to dominate and at higher enzyme activity, the fractionation values are overestimated if the instrument response time of the MIMS system is exceeded (see discussion on sources of error below). The background represents the drawdown of O_2 in the closed cuvette and monitors the pervaporation of the O_2 molecules across the LDPE membrane into the high vacuum of the mass spectrometer system. The background rate of O_2 consumption was carefully tuned by membrane selection: polymer type, thickness, surface area.

Data Analysis of Reaction. Examples of the data and its analysis from liquid (glycolate oxidase reaction) and gaseous (soybean leaf disc respiration) reactions is shown (Figure 2). One of the advantages of the MIMS approach is that continuous data can be produced for the concentration of each O_2 isotopologue of interest, allowing data analysis in a number of ways. Recent consideration of methods to analyze kinetic isotope effects from different forms of the Rayleigh distillation equation have concluded that the best estimates come from the slope of a plot of ln(R) versus ln(C), where R and C are the isotopic ratio $^{18}O/^{16}O$ and the concentration of O_2, respectively.[13,14] The kinetic isotope effect ($R_s/R_p = \alpha$) can be obtained as

$$\alpha = 1/(\text{slope} + 1)$$

The commonly used discrimination value (Δ) can be obtained from this as

$$\Delta = (\alpha - 1) \times 1000$$

Another advantage of this approach is that calibration of mass intensities is not required and the data analysis becomes unit-less, i.e., discrimination values can simply be derived from the slope of a ln(mass 34/mass 32) vs ln(mass 32) plot (see Supporting Information).

A plot of the data (Figures 2c,d) shows that a good linear fit is obtained with less than 4 parts per thousand error on the slope regression value. Characteristic slopes for O_2 consumption in each assay are shown (Figures 2e,f). For the glycolate oxidase assay, stable estimates of the slope are obtained after about 100 s of assay, which is when about 20% of the O_2 is consumed. For the gaseous leaf disc assay, stable values are obtained after 300−400 s of assay, which again corresponds to about 20% consumption. In a typical analysis, discrimination values are derived from data between 20 and 50% consumption of O_2.

Oxygen Consuming Assays. Purified enzyme assays were conducted using air saturated solutions, containing O_2 at natural abundance isotope enrichment.

Glucose oxidase (Sigma-Aldrich, lyophilized powder, *Aspergillus niger*, EC 1.1.3.4) was assayed in 100 mM HEPES, pH 7.4, in the presence of 2 mM glucose and approximately 25 units mL^{-1} catalase.

Glycolate oxidase (Sigma-Aldrich, NH_4SO_4 suspension, spinach, EC 1.1.3.15) was assayed in 50 mM Tris, pH 8.3, in the presence of 85 μM FMN and 6 mM glycolate.

Xanthine oxidase (Sigma-Aldrich, NH_4SO_4 suspension, buttermilk, EC 1.17.3.2) was assayed in 100 mM HEPES, pH 7.4, in the presence of 1 mM xanthine and approximately 25 units mL^{-1} catalase.

Choline oxidase (Sigma-Aldrich, lyophilized powder, *Alcaligenes* species, EC 1.1.3.17) was assayed in 100 mM Tris pH 8, 1 mM EDTA, 10 mM Choline chloride and approximately 25 units mL^{-1} catalase. Choline chloride was dissolved in methanol prior to use.

RuBisCO (purified from spinach in house,[15] EC 4.1.1.39) was assayed in 100 mM HEPES, pH 8.0, 20 mM $MgCl_2$, no added inorganic carbon. Assay was started by the addition of enzyme which has been preactivated in assay buffer in the presence of 10 mM $NaHCO_3^-$ on ice.

L-amino acid oxidase (Sigma-Aldrich, lyophilized powder, snake venom, EC 1.4.3.2) was assayed in 100 mM HEPES pH 7.4, 1 mM phenylalanine, 25 units mL^{-1} catalase.

D-amino acid oxidase (Sigma-Aldrich, lyophilized powder, porcine kidney, EC 1.4.3.3) was assayed in 100 mm Tris, pH 8.2, 20 mM D-alanine, 25 units mL^{-1} catalase.

It should be noted that while catalase may, in principle, bias the discrimination values, experiments with glucose oxidase employing horse radish peroxidase with guaiacol to scavenge H_2O_2 gave essentially identical discrimination values (data not shown). Furthermore, the discrimination value of glycolate oxidase is reportedly unchanged in the presence and absence of catalase;[10] similar results were obtained in this study (data not shown).

Cytochrome *c* oxidase (purified from bovine heart[16] and *Rhodobacter sphaeroides*[17] in house, EC 1.9.3.1) was assayed in 100 mM HEPES pH 7.4 with 25 μM cytochrome *c* (equine heart, Sigma-Aldrich) and 5 mM ascorbic acid as electron donors.

Isolated mitochondrial assays were also conducted using air-saturated solutions containing O_2 at natural abundance isotope enrichment. Purification of mitochondria from soybean cotyledons and addition of substrates and inhibitors were as described[18] and all assays were performed in 300 mM sucrose, 5 mM KH_2PO_4, 10 mM TES pH 7.2, 10 mM NaCl, 2 mM $MgSO_4$, 0.1% BSA.

Cytochrome *c* oxidase (EC 1.9.3.1) was measured in intact mitochondria using succinate (10 mM) as a respiratory substrate and *n*-propyl gallate (0.05 mM) to inhibit the alternative pathway.

Alternative oxidase (EC 1.10.3.11) was measured in intact mitochondria using succinate (10 mM) as respiratory substrate and KCN (0.05 mM) to inhibit cytochrome *c* oxidase.

Uninhibited respiration by mitochondria was measured using succinate (10 mM) as a respiratory substrate together with 0.1 mM ATP and as external NADH-dependent respiration using 1 mM NADH. Pyruvate (0.1 mM) was added in separate

dx.doi.org/10.1021/ac501086n | *Anal. Chem.* XXXX, XXX, XXX−XXX

Table 1. Measurements of Oxygen Kinetic Isotope Discrimination Values (Δ) for Various Liquid and Gaseous Reactions Catalyzed by Purified Enzymes, Isolated Mitochondria and Leaf Discs[a]

sample	discrimination (‰)	reported values (‰)
liquid phase: purified enzymes [source]		
glycolate oxidase [spinach]	23.0 ± 0.9	22.9[b], 22.7[c]
xanthine oxidase [buttermilk]	31.3 ± 0.5	26.3 ± 5.6[d]
glucose oxidase [*Aspergillus niger*]	31.6 ± 0.5	27−28[e]
RuBisCO oxygenase [spinach leaves]	22.9 ± 0.4	21.3[c]
Choline oxidase [*Alcaligenes* species]	19.9 ± 1.4	this paper only
L-amino acid oxidase [snake venom]	45.6 ± 0.3	this paper only
D-amino acid oxidase [porcine kidney]	50.3 ± 1.7	this paper only
cytochrome *c* oxidase [*Rhodobacter sphaeroides*]	18.6 ± 0.5	this paper only
cytochrome *c* oxidase [bovine heart]	22.1 ± 1.1	this paper only
liquid phase - soybean mitochondria [substrates and inhibitors]		
alternative oxidase [succinate + KCN]	27.3 ± 0.4	31.6[b]
cytochrome oxidase [succinate + nPG]	20.2 ± 0.3	21.0[b]
mitochondrial respiration [succinate + ATP]	23.4 ± 0.2	24.0 ± 0.2[b]
mitochondrial respiration [NADH]	21.9 ± 0.2	21.9 ± 0.4[b]
mitochondrial respiration [NADH + pyruvate]	23.7 ± 0.3	26.0 ± 0.3[b]
gas phase - soybean leaf discs [treatment]		
leaf respiration [control]	23.6 ± 0.3	23.4 ± 0.7[f]
leaf respiration [+ KCN]	29 ± 1	29.3[f]

[a]Values are presented for measurements made in the current study and compared with values previously reported in the literature. Measurements in this study are the means plus standard errors of five replicate assays. [b]Ref 8. [c]Ref 10. [d]This paper, determined using conventional CO_2 equilibration method. [e]Ref 20. [f]Refs 7,21.

NADH-dependent respiratory assays to activate alternative oxidase and shift the flux distribution between the two oxidase toward AOX.[19] Whole tissue respiratory assays in gas phase were performed in leaf discs from soybean seedlings. Six to eight discs (128.93 mm^2 each) were placed in the gas phase cuvette above filter paper dampened with 0.1 M NaOH. Discrimination measurements were taken after the cuvette was sealed from the external atmosphere. Treatments of leaf discs with KCN were performed in separate containers prior to the measurements. KCN was administered in a 15 mL sealed vessel by placing the leaf discs above a pad of filter paper saturated with 1 M KCN, 10 mM TES, pH 7.0 for 15 min. Discs were then transferred to the reaction chamber. Soybeans were grown in a naturally lit glasshouse on vermiculite media and leaf discs were cut from primary leaves 2 weeks after germination.

RESULTS

Measurement of O_2 Consuming Reactions by Purified Oxidases. The O_2 isotope discrimination values for a range of O_2 consuming reactions, some previously characterized,[7,8,10,20−23] were determined and presented alongside previous values in the literature (Table 1). The purified enzymes reported in Table 1 are mostly flavin-containing oxidases, except for RuBisCO and the copper containing cytochrome *c* oxidases from bacteria, mammals and plants. For the most part, the discrimination factors/^{18}O KIEs agree with values in the literature, which were determined using a specialized vacuum apparatus to prepare CO_2 samples from purified unreacted O_2 prior to analysis by isotope ratio mass spectrometry (IRMS). MIMS measurements on RuBisCO are increased by 1.6 parts per thousand. Values for glucose oxidase are ca. 4 parts per thousand higher than those measured earlier.[20,22,23] MIMS data for xanthine oxidase indicate a value of approximately 30‰, which is 5 parts per thousand greater than those determined previously. In this case similar ^{18}O KIEs are expected for superoxide production in the first irreversible step of the oxidative half-reaction. Another flavoprotein, choline oxidase exhibits and ^{18}O KIE ca. 20‰, which is close to that observed for glycolate oxidase, whereas different mechanism of O_2 reduction has been considered.[24] Two surprising results were obtained for the D- and L-amino acid oxidases, which are both in excess of 45 ‰ and larger than any other O_2-consuming enzyme examined to date using competitive oxygen isotope fractionation.

Oxygen Consumption by Mixed Oxidase Systems in Liquid and Gas Phase. The dual oxidases of plant mitochondria, which operate at approximately equal rates in soybean tissues,[7,8] provided a convenient system to study kinetic isotope effects in biological tissues and the impact of respiratory inhibitors. Table 1 shows that uninhibited plant mitochondrial respiration driven by succinate in liquid phase yielded values halfway between those for cytochrome and alternative oxidases. Addition of pyruvate to activate alternative oxidase during NADH oxidation,[18,19] noticeably increased O_2 isotope discrimination, as the alternative oxidase was further engaged (Table 1). In gas phase, the two oxidases could also be observed to be operating together and KCN gassing of leaf tissue to inhibit cytochrome *c* oxidase in vivo shifted isotope discrimination toward that of the alternative oxidase (Table 1).

Assessment of Parameters That Influence Isotope Enrichment. *Mass Zeros.* The assays (Figure 2a−d) require no machine calibration relating to mass intensities as the data analysis is unit-less, but the final analysis is very sensitive to the estimate of the zero values for each mass. The mass values used for calculation (Figure 2a−d) are the absolute mass intensities minus the system zero value, which exists in the absence of any O_2-derived species in the cuvette. Positive zero values arise both from the amplification system as well as small O_2 leaks into the vacuum of the mass spectrometer. As we are measuring changes in isotope ratios, with errors on the order of parts per thousand, an incorrect zero can bias the discrimination value quite dramatically. An example of this is shown (Figure 3) for the

dx.doi.org/10.1021/ac501086n | Anal. Chem. XXXX, XXX, XXX−XXX

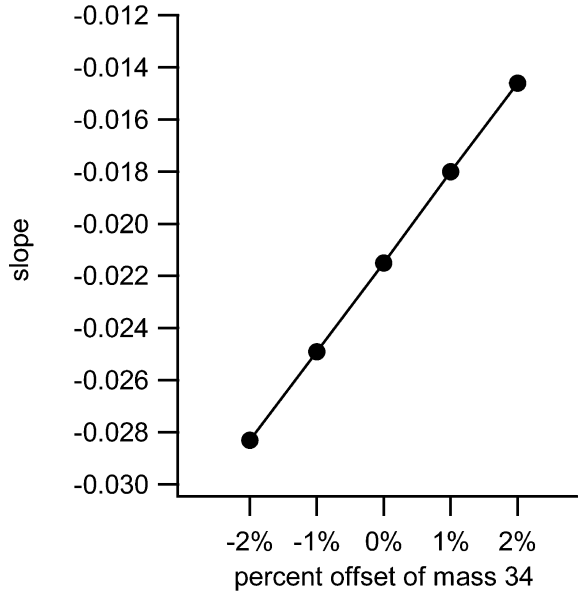

Figure 3. The effect of a zero offset applied to mass 34 on the calculated slope for the glycolate oxidase reaction shown in Figure 2a. Mass 34 data obtained in Figure 2a was adjusted assuming zero values that differed from the correct value by the offset percentage shown on the *x*-axis and the data replotted as in Figure 2a. Slopes for the replotted data are reported.

glycolate oxidase assay, a 1% error in the estimation of the mass 34 zero has about a 16% effect on the slope of the plot (Figure 2c), and thus on discrimination estimates. We found that a number of methods could be used to establish an accurate and reproducible zero value. This included the addition of dithionite to liquid in the cuvette, flushing continuously with oxygen-free nitrogen, or isolation of the cuvette from the mass spectrometer source by a valve located adjacent to the reaction cuvette. As the last technique was the most convenient and subject to least error we regularly used this to measure the mass 32 and mass 34 zero values. These zero values were subtracted from each mass measurement during the experiment. These values were very reproducible and remained constant for several hours of experiments and were checked every 2 hours to monitor any drift.

Consumption of O_2 by the Membrane. As mentioned above, another major source of error in liquid experiments arises from the consumption of gas by the vacuum pump interfaced with the mass spectrometer. Excessively permeable membranes present an intrinsic isotopic fractionation parameter that complicates analysis. However, we have found that this can be ignored if the background rates of O_2 consumption in the cuvette are minimized (Figure 2a). In the simplest analysis, there are two competing O_2 consumption reactions in this MIMS approach, each with an intrinsic discrimination value. One is the O_2 consumption by the enzyme assay (Δ_{enzyme}) and the second is the consumption via the membrane ($\Delta_{membrane}$) into the mass spectrometer vacuum. The measured discrimination value is then the total discrimination (Δ_{total}) of the two competing reactions and is related by the following equation, where A is the partition toward the enzyme consumption reaction.[7]

$$\Delta_{total} = A \times \Delta_{enzyme} + (1 - A) \times \Delta_{membrane}$$

It is possible, in principle, to obtain the intrinsic enzyme discrimination (Δ_{enzyme}) value by linearizing the equation above based on assays with a range of enzyme concentrations. However, in practice, it is found that there is a large error in estimating the enzyme partition that precludes estimation of meaningful intrinsic enzyme fractionation values. In addition, systematic effects such as slow leak of O_2 are not taken into account. Therefore, the approach that we have adopted is to simply minimize the O_2 consumption by the membrane, i.e., $A \approx 1$, hence

$$\Delta_{total} \approx \Delta_{enzyme}$$

This is achieved by fixing the rate of enzyme reaction for various enzymes, which have different turnover rates, via adjustment of enzyme concentration during assays (refer to Assay Procedures in Materials and Methods).

The effect of membrane consumption is simulated based on the partitioning equation above for the glycolate oxidase reaction and is presented (Figure 4). It is clear that Δ_{total} will be

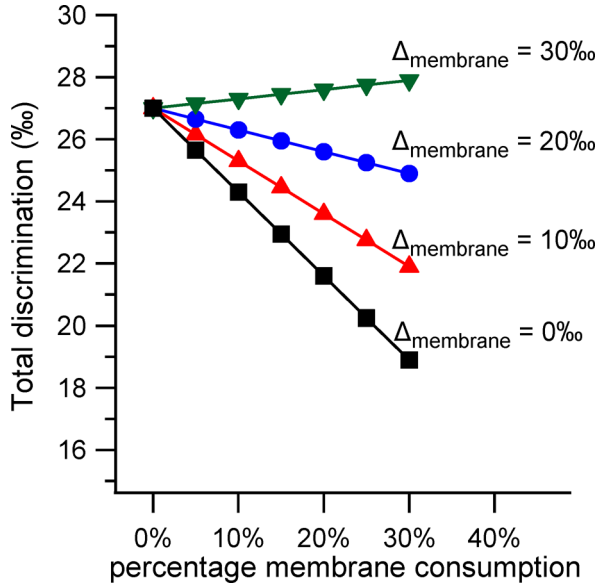

Figure 4. Effect of the rate of membrane O_2 consumption and its isotope discrimination on the measured O_2 isotope discrimination of a glycolate oxidase reaction. The data were calculated by assuming that the membrane and the enzymatic reaction were two competing O_2 consuming reactions.[7]

significantly biased, irrespective of value of $\Delta_{membrane}$, when the percentage of O_2 consumption by membrane is high. Using a permeable membrane that has minimal consumption but still allows sufficient signal intensity, along with increasing the volume of the assays to minimize the membrane consumption per unit volume of reaction, minimizes this error. We used a low density polyethylene membrane (ca. 43 μm thick), which caused less than 5% O_2 consumption during the assay period (95% partitioning toward enzyme reaction) and its O_2 discrimination was estimated as 5−7 parts per thousand.

DISCUSSION

New Approach to Measuring O_2 Isotope Discrimination. From a technical perspective, the liquid and gaseous techniques described here represent reasonably quick and easy approaches to determining O_2 isotope discrimination values for

dx.doi.org/10.1021/ac501086n | *Anal. Chem.* XXXX, XXX, XXX−XXX

various O_2 consuming processes. While modification of gas inlets of standard isotope ratio mass spectrometers is required, the approach offers accuracy similar to that of standard O_2 isotope discrimination measurement techniques (Table 1). The most significant advantage of the MIMS compared to traditional approaches is that gas extraction and purification from liquid assays is not required, allowing assays to be completed and analyzed in a time window similar to the assay period, thus enabling a higher throughput of samples. This may be important for screening large populations of organisms for mutant or natural variants of oxidases. Studies of many different O_2 consuming reactions and enzymes can be easily accomplished (Table 1). We show its use and accuracy in analysis of purified oxidases, subcellular fractions (isolated mitochondria) and whole tissue samples, exemplifying the broad applicability of this technique for different types and complexities of samples.

The most significant limitation of the approach is primarily associated with the determination of the correct cuvette zero value (Figure 3). Previous methods for isotope analysis have measured O_2 samples that have been more concentrated and produced a much higher O_2 signal-to-zero value ratio compared with measurements reported here, which meant errors due to machine zero levels were much less significant. Nonetheless, this appears to be readily accommodated if a convenient method can be established to measure the cuvette zero, such as periodically isolating the cuvette from the mass spectrometer. Using a gas permeable membrane with a higher permeability can also reduce this potential error, but, as discussed above, the membrane gas consumption must be minimized to reduce its potential error contribution (Figure 4).

Membrane inlet mass spectrometry has had many applications in the measurement of biological gas isotope fluxes.[25] The use described here for real-time isotope discrimination opens up a new dimension in the applications window for this technology. Indeed, we have previously shown that similar approaches to those described here can also be applied to CO_2 isotope discrimination reactions.[14] However, in this instance, the problem of zero values is exacerbated because of lower signal levels and production of CO_2 by the source filament. Despite this, the same approach can be made to work well for CO_2 consuming enzyme reactions, offering an easy and reproducible method for what was previously a very time-consuming technical process. We have used the approach described here for O_2 gas consuming reactions to study of changes in cytochrome oxidase and alternative oxidase in cold acclimating leaves of *Arabidopsis thaliana*.[26] The results obtained allowed the analysis of O_2 isotope discrimination of the respiration of many different leaf samples over a period of several weeks, together with estimates of net O_2 uptake flux. This frequency of sampling and analysis has not been possible previously and provides a widely applicable approach to study multiple oxidases in biological systems.

Insights into Enzymatic Mechanism. Oxygen isotope discrimination measurements such as those reported here can give insights into the kinetic mechanism of enzyme reactions. The cytochrome *c* oxidase[8] and glycolate oxidase[8,10] exhibit discrimination factors that are essentially competitive kinetic isotope effects (^{18}O KIE). These ^{18}O KIEs are, by definition, the ratio of $k_{cat}/K_M(^{16,16}O_2)$ relative to $k_{cat}/K_M(^{16,18}O_2)$. These bimolecular rate constants are defined by the enzymes' kinetic mechanisms.[27] In cases where oxidases react by "ping-pong" type kinetic mechanisms, the ^{18}O KIE is a probe of O_2 reduction independent of cosubstrate oxidation; whereas in the oxygenase RuBisCO, the ^{18}O KIE is controlled by O_2 uptake in equilibrium with the activated substrate or a common intermediate. These differences in kinetic mechanisms have implications for the electron transfer mechanism by which O_2 reduction takes place (vide infra).

The magnitude of competitive ^{18}O KIEs can provide clues as to the nature of the electron transfer reactions occurring in O_2-consuming enzymes. Previously, equilibrium isotope effects (^{18}O EIE) were suggested to be upper limits for the ^{18}O KIEs on reactions that involve coordination of O_2 to a reduced transition metal.[2,28,29] It has since been shown that ^{18}O KIEs on O_2 consumption can exceed the corresponding ^{18}O EIEs when reactions involve significant mass-dependence of the reaction coordinate motion.[1,30,31]

It is generally considered that flavoprotein oxidases reduce O_2 by the transfer of electrons by outer-sphere, stepwise processes.[32,33] The first rate-limiting electron transfer step is assumed to produce a caged radical pair consisting of the superoxide anion and the flavin semiquinone. The second reductive step can proceed by multiple pathways, resulting in generation of hydrogen peroxide. For glucose oxidase, the magnitude of the ^{18}O KIE has been reproduced using quantum chemical calculations on the conversion of O_2 to $O_2^{\bullet-}$.[20] The calculations resemble the Franck−Condon overlap factor, depending on the change in vibrational stretching frequency and the O−O bond distance.

On the basis of the above discussion, the O_2 discrimination observed by the D- and L-amino acid oxidases (Table 1) suggest the possibility that O_2 may be reduced beyond the level of superoxide possibly to a deprotonated peroxide intermediate. In this case, the reaction may involve a reversible pre-equilibrium electron transfer followed by an irreversible net hydrogen atom transfer from the flavin semiquinone cofactor. The ^{18}O KIE would thus be the product of a pre-equilibrium isotope effect of 1.03 on reversible electron transfer and a normal kinetic isotope effect approaching 1.02 on irreversible proton-coupled electron transfer.[31] However, current reaction mechanism studies of both these enzymes have not specifically considered the oxygen activation step in detail.[34−36] Though no evidence for a peroxyflavin intermediate has been obtained to date,[33] the similar values for both amino acid oxidases are in agreement with the notion of Massey and Curti[34] that the two types of oxidases proceed by similar O_2 activation pathways. Moreover, the large isotope discrimination raises questions concerning the maximum ^{18}O KIE observable for rate-limiting electron transfer to O_2, which would be expected to result from a late transition state and extensive O−O bond displacement.[23] This phenomenon could be distinguished from the multi-electron transfer reaction, which would be expected to exhibit a solvent deuterium kinetic isotope effect on $k_{cat}/K_M(O_2)$.

■ ASSOCIATED CONTENT

Supporting Information

Derivation of equation for determining KIE using MIMS data based on the Rayleigh distillation equation. This material is available free of charge via the Internet at http://pubs.acs.org.

■ AUTHOR INFORMATION

Corresponding Authors

*M. H. Cheah. E-mail: michael.cheah@anu.edu.au. Phone: (612) 6125-0276.

*M. R. Badger. E-mail: murray.badger@anu.edu.au. Phone: (612) 6125-3741.

Funding

We acknowledge funding from the Australian Research Council (FT110100242, CE0561495, DP120100872).

Notes

The authors declare no competing financial interest.

■ ACKNOWLEDGMENTS

Our close friend and colleague Warwick Hillier passed away on January 10, 2014. He will be greatly missed.

■ ABBREVIATIONS

IRMS	isotope ratio mass spectrometer
MIMS	membrane inlet mass spectrometry
AOX	alternative oxidase
CcO	cytochrome *c* oxidase
KIE	kinetic isotope effect
HEPES	4-(2-hydroxyethyl)piperazine-1-ethanesulfonic acid
Tris	2-amino-2-hydroxymethylpropane-1,3-diol
TES	2-[[1,3-dihydroxy-2-(hydroxymethyl)propan-2-yl]-amino]ethanesulfonic acid
BSA	bovine serum albumin
nPG	*n*-propyl gallate
LDPE	low density polyethylene
PFA	perfluoroalkoxy polymer
FMN	flavin mononucleotide

■ REFERENCES

(1) Liu, Y.; Mukherjee, A.; Nahumi, N.; Ozbil, M.; Brown, D.; Angeles-Boza, A. M.; Dooley, D. M.; Prabhakar, R.; Roth, J. P. *J. Phys. Chem. B* **2013**, *117*, 218−229.
(2) Roth, J. P. *Acc. Chem. Res.* **2009**, *42*, 399−408.
(3) Tian, G. C.; Klinman, J. P. *J. Am. Chem. Soc.* **1993**, *115*, 8891−8897.
(4) Mirica, L. M.; McCusker, K. P.; Munos, J. W.; Liu, H.-w.; Klinman, J. P. *J. Am. Chem. Soc.* **2008**, *130*, 8122−8123.
(5) Smirnov, V. V.; Brinkley, D. W.; Lanci, M. P.; Karlin, K. D.; Roth, J. P. *J. Mol. Catal. A: Chem.* **2006**, *251*, 100−107.
(6) Guy, R. D.; Berry, J. A.; Fogel, M. L.; Hoering, T. C. *Planta* **1989**, *177*, 483−491.
(7) Robinson, S. A.; Ribas-Carbo, M.; Yakir, D.; Giles, L.; Reuveni, Y.; Berry, J. A. *Aust. J. Plant Physiol.* **1995**, *22*, 487−496.
(8) Ribas-Carbo, M.; Berry, J. A.; Yakir, D.; Giles, L.; Robinson, S. A.; Lennon, A. M.; Siedow, J. N. *Plant Physiol.* **1995**, *109*, 829−837.
(9) Badger, M. R. *Annu. Rev. Plant Physiol. Plant Mol. Biol.* **1985**, *36*, 27−53.
(10) Guy, R. D.; Fogel, M. L.; Berry, J. A. *Plant Physiol.* **1993**, *101*, 37−47.
(11) Helman, Y.; Barkan, E.; Eisenstadt, D.; Luz, B.; Kaplan, A. *Plant Physiol.* **2005**, *138*, 2292−2298.
(12) Ribas-Carbo, M.; Robinson, S. A.; Gonzalez-Meler, M. A.; Lennon, A. M.; Giles, L.; Siedow, J. N.; Berry, J. A. *Plant Cell Environ.* **2000**, *23*, 983−989.
(13) Scott, K. M.; Lu, X.; Cavanaugh, C. M.; Liu, J. S. *Geochim. Cosmochim. Acta* **2004**, *68*, 433−442.
(14) McNevin, D. B.; Badger, M. R.; Kane, H. J.; Farquhar, G. D. *Funct. Plant Biol.* **2006**, *33*, 1115−1128.
(15) Hall, N. P.; Tolbert, N. E. *FEBS Lett.* **1978**, *96*, 167−169.
(16) Yoshikawa, S.; Choc, M. G.; O'Toole, M. C.; Caughey, W. S. *J. Biol. Chem.* **1977**, *252*, 5498−5508.
(17) Gennis, R. B.; Casey, R. P.; Azzi, A.; Ludwig, B. *Eur. J. Biochem.* **1982**, *125*, 189−195.
(18) Hoefnagel, M. H. N.; Millar, A. H.; Wiskich, J. T.; Day, D. A. *Arch. Biochem. Biophys.* **1995**, *318*, 394−400.
(19) Millar, A. H.; Hoefnagel, M. H. N.; Day, D. A.; Wiskich, J. T. *Plant Physiol.* **1996**, *111*, 613−618.
(20) Su, Q. J.; Klinman, J. P. *Biochemistry* **1999**, *38*, 8572−8581.
(21) Robinson, S. A.; Yakir, D.; Ribas-Carbo, M.; Giles, L.; Osmond, C. B.; Siedow, J. N.; Berry, J. A. *Plant Physiol.* **1992**, *100*, 1087−1091.
(22) Roth, J. P.; Klinman, J. P. *Proc. Natl. Acad. Sci. U. S. A.* **2003**, *100*, 62−67.
(23) Roth, J. P.; Wincek, R.; Nodet, G.; Edmondson, D. E.; McIntire, W. S.; Klinman, J. P. *J. Am. Chem. Soc.* **2004**, *126*, 15120−15131.
(24) Rungsrisuriyachai, K.; Gadda, G. *Biochemistry* **2008**, *47*, 6762−6769.
(25) Beckmann, K.; Messinger, J.; Badger, M. R.; Wydrzynski, T.; Hillier, W. *Photosynth. Res.* **2009**, *102*, 511−522.
(26) Armstrong, A. F.; Badger, M. R.; Day, D. A.; Barthet, M. M.; Smith, P. M. C.; Millar, A. H.; Whelan, J.; Atkin, O. K. *Plant Cell Environ.* **2008**, *31*, 1156−1169.
(27) Roth, J. P. *Curr. Opin. Chem. Biol.* **2007**, *11*, 142−150.
(28) Lanci, M. P.; Brinkley, D. W.; Stone, K. L.; Smirnov, V. V.; Roth, J. P. *Angew. Chem., Int. Ed.* **2005**, *44*, 7273−7276.
(29) Lanci, M. P.; Roth, J. P. *J. Am. Chem. Soc.* **2006**, *128*, 16006−16007.
(30) Ashley, D. C.; Brinkley, D. W.; Roth, J. P. *Inorg. Chem.* **2010**, *49*, 3661−3675.
(31) Huff, G. S.; Doncheva, I. S.; Brinkley, D. W.; Angeles-Boza, A. M.; Mukherjee, A.; Cramer, C. J.; Roth, J. P. *Biochemistry* **2011**, *50*, 7375−7389.
(32) Mattevi, A. *Trends Biochem. Sci.* **2006**, *31*, 276−283.
(33) Massey, V. *Int. Congr. Ser.* **2002**, *1233*, 3−11.
(34) Massey, V.; Curti, B. *J. Biol. Chem.* **1967**, *242*, 1259−1264.
(35) Tishkov, V. I.; Khoronenkova, S. V. *Biochemistry (Moscow)* **2005**, *70*, 40−54.
(36) Moustafa, I. M.; Foster, S.; Lyubimov, A. Y.; Vrielink, A. *J. Mol. Biol.* **2006**, *364*, 991−1002.